



Scholars Research Library

Der Pharmacia Lettre, 2014, 6 (1):95-104  
(<http://scholarsresearchlibrary.com/archive.html>)



## A quantum-chemical analysis of the relationships between hCB2 cannabinoid receptor binding affinity and electronic structure in a family of 4-oxo-1,4-dihydroquinoline-3-carboxamide derivatives

Juan S. Gómez-Jeria

*Quantum Pharmacology Unit, Department of Chemistry, Faculty of Sciences, University of Chile, Las Palmeras, Santiago, Chile*

---

### ABSTRACT

*The present paper presents and discusses the relationship between molecular-electronic structure and hCB2 receptor binding affinity of a family of 4-oxo-1,4-dihydroquinoline-3-carboxamide derivatives with a formal method recently enlarged by the author. The electronic structures of all molecules were calculated within Density Functional Theory at the B3LYP/6-311g(d,p) level. We obtained a statistically significant equation relating the variation of hCB2 receptor binding affinities with the variation of a definite set of local atomic reactivity indices. For the case analyzed here, the interaction of the molecules with the hCB2 receptor is mainly charge-controlled. More studies of different series are needed to expand our knowledge of the hCB2 interaction pharmacophore. The common skeleton hypothesis seems to work well enough to be applied in this kind of studies.*

---

### INTRODUCTION

Before the 1980s, it was frequently speculated that cannabinoids produced their physiological and behavioral effects by means of nonspecific interactions with cell membranes, instead of interacting with specific membrane-bound receptors. The discovery of the first cannabinoid receptors in the 1980s helped to decide this dispute. These receptors are common in animals, and have been found in mammals, reptiles, birds and fishes. There are at least two kinds of cannabinoid receptors called CB1 and CB2 [1,2]. Ligands activating these G protein-coupled receptors comprise the phytocannabinoid  $\Delta^9$ -tetrahydrocannabinol, a variety of synthetic compounds, and endogenous compounds (endocannabinoids). The CB2 receptor is expressed mainly in the cells and tissues of the immune system including thymus, tonsils, B and T cells, macrophages, monocytes and NK cells and, to a far lesser amount, in brain. In both central nervous system and peripheral tissues, the CB2 receptor is up-regulated near the beginning of inflammatory events [3,4]. Several kinds of ligands bind to the CB2 receptor [5]. They have been classified as classical cannabinoids, non-classical cannabinoids, cannabimimetic indoles, pyrazoles and 2-oxoquinolines.

The exact knowledge of the mode of binding of these different ligands to cannabinoid receptors is of paramount importance for designing new ligands with enhanced receptor affinity. The apparently very distinct chemical structure of the ligands binding to these receptors makes it necessary to carry out extensive studies of several different families of molecules in order to detect their common features. In general terms, this observation is still valid today, not only for cannabinoids but for all molecules presenting any kind of biological activity. These studies must be carried out with model-based methods [6] able to deal with the fact that the molecular properties that are directly responsible for the molecular interactions leading to the pharmacological effect are encoded in the entire molecular structure [7]. Usually experimentalists publish papers containing one or more Tables with experimental results (receptor affinities, anti-proliferative activity, toxicity, etc.) of a group of molecules. In the main body of the paper they transform these Tables into a list of requirements for enhanced or diminished activity. These lists of

requirements are included within the broadest meaning of “structure-activity relationships” (SAR) but, technically, they are no more than a verbal translation of the results reported in these Tables. At most, these lists are vaguely supported by general statements taken from organic chemistry or related areas.

To date, only three quantum-chemical studies correlating the full description of the entire molecules exhibiting a biological activity have been published in the cannabinoid field. By description we mean the account, in quantum-chemical terms, of the reactivity of all atoms forming the molecule and the geometric effects of the substituents. It is important to stress that a necessary condition is that this description must appear in a formal manner within a model linking biological activity and electronic structure [6]. The first paper analyzed the CB1- and CB2-mediated inhibition of adenylyl cyclase by a group of classical cannabinoid derivatives [8]. In the second one we presented structure-receptor affinity relationships for the *in vitro* interaction of a group of classical, indole-derived and aminoalkylindole-derived cannabinoids [9]. On the basis of these results a new molecule was proposed that should help to distinguish between both receptor sites. The results of these two studies are very encouraging taking into account that the numerical values for the local atomic descriptors were obtained with a semiempirical method. In the most recent study a search was carried out to find relationships between hCB1 and hCB2 receptor binding affinity and molecular structure for a group of 1-aryl-5-(1*H*-pyrrol-1-yl)-1*H*-pyrazole-3-carboxamides [10]. The present paper shows and discusses the relationships between molecular-electronic structure and hCB2 receptor binding affinity of a family of 4-oxo-1,4-dihydroquinoline-3-carboxamide derivatives [11]. As the methods employed here are the same used in the previous paper [10], a secondary goal is to analyze the feasibility of a comparison between the results of both. For a short review of earlier theoretical studies see Ref. [10]. For historical aspects of cannabis see Refs. [12-18]. For the use of cannabis and chemicals obtained from it for antidiabetic activity and weight loss in obese patients see Refs. [19, 20].

## MATERIALS AND METHODS

### METHODS, MODELS AND CALCULATIONS

#### The method

Given that the model-based method relating drug-receptor equilibrium constants with molecular structure has been described in great detail elsewhere, we present here only the final results [9,21-30]. The drug-receptor affinity constant,  $\log K_i$ , is a linear function of several local atomic reactivity indices (LARIs) and has the following general form:

$$\begin{aligned} \log K_i = & a + bM_{D_i} + c \log \left[ \sigma_{D_i} / (ABC)^{1/2} \right] + \sum_j \left[ e_j Q_j + f_j S_j^E + s_j S_j^N \right] + \\ & + \sum_j \sum_m \left[ h_j(m) F_j(m) + x_j(m) S_j^E(m) \right] + \sum_j \sum_{m'} \left[ r_j(m') F_j(m') + t_j(m') S_j^N(m') \right] + \\ & + \sum_j \left[ g_j \mu_j + k_j \eta_j + o_j \omega_j + z_j \zeta_j + w_j Q_j^{\max} \right] \end{aligned} \quad (1)$$

where  $M$  is the drug's mass,  $\sigma$  its symmetry number and  $ABC$  the product of the drug's moments of inertia about the three principal axes of rotation.  $Q_i$  is the net charge of atom  $i$ ,  $S_i^E$  and  $S_i^N$  are, respectively, the total atomic electrophilic and nucleophilic superdelocalizabilities of Fukui *et al.*,  $F_{i,m}$  ( $F_{i,m'}$ ) is the Fukui index of the occupied (empty) MO  $m$  ( $m'$ ) located on atom  $i$ .  $S_i^E(m)$  is the atomic electrophilic superdelocalizability of MO  $m$  on atom  $i$ , etc. The total atomic electrophilic superdelocalizability of atom  $i$  corresponds to the sum over occupied MOs of the  $S_i^E(m)$ 's and the total atomic nucleophilic superdelocalizability of atom  $i$  is the sum over empty MOs of the  $S_i^N(m)$ 's. The last bracket of the right side of Eq. 1 contains new local atomic reactivity indices obtained directly from Molecular Orbital Theory by an approximate reorganization of part of the remaining terms of the series expansion used in the model [31,32].

The moment of inertia term can be expressed as:

$$\log \left[ (ABC)^{-1/2} \right] = \sum_t \sum_t m_{i,t} R_{i,t}^2 = \sum_t O_t \quad (2)$$

where the summation over  $t$  is over the various substituents of the molecule,  $m_{i,t}$  is the mass of the  $i$ -th atom belonging to the  $t$ -th substituent,  $R_{i,t}$  being its distance to the atom to which the substituent is bonded. A molecular property was thus transformed into a sum of substituent properties. We proposed that the appearance of any  $O_t$  in a

QSAR equation is related to its influence on the fraction of molecules attaining the correct orientation to interact with the receptor. We called the  $O_i$ 's Orientational Parameters [24,25]. In summary, for  $n$  molecules we have a set of  $n$  simultaneous equations 1. This system of simultaneous equations holds for the atoms of the molecule directly perturbed by their interaction with the receptor. Combined with the standard multiple-regression techniques, these equations can be usefully applied to estimate the relative variation of  $\log K_i$  in terms of the variation of the values of a definite set of LARIs. Here statistical analysis is used only to find the best structure-activity relationships. This method has been successfully applied to many different kinds of receptors and ligands [9,10,21,24, 26-28,30,33-43].

### Selection of the experimental data

The experimental data employed in this study are to the receptor binding affinities measured in CHO cells transfected with the cDNA sequences encoding the human CB2 cannabinoid receptor (hCB2). Molecules were selected from a set reported in Ref. [11]. The molecules are shown in Fig. 1 and Table 1. Figure 2 shows the numbering of atoms used in the linear multiple regression analysis (LMRA).

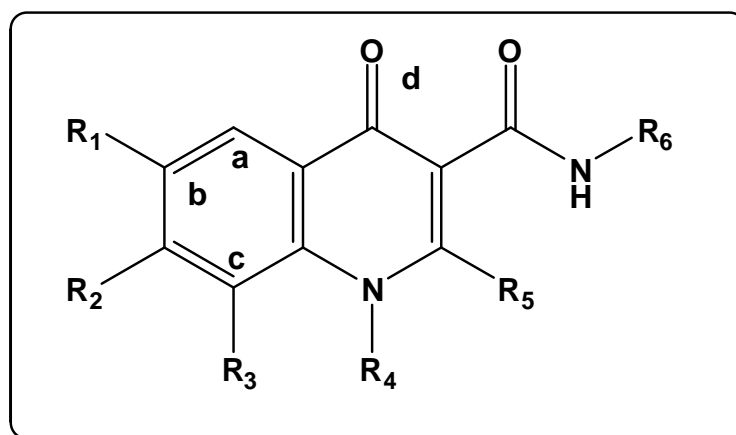


Figure 1. 4-oxo-1,4-dihydroquinoline-3-carboxamide derivatives.

Table 1. 4-oxo-1,4-dihydroquinoline-3-carboxamide derivatives and their hCB2 receptor binding affinity\*.

Mol.	R <sub>1</sub>	R <sub>2</sub>	R <sub>3</sub>	R <sub>4</sub>	R <sub>5</sub>	R <sub>6</sub>	log K <sub>i</sub> (nM)
1	H	H	H	4-fluorobenzyl	H	1-(3,5-dimethyl)adamantanyl	1.92
2	H	H	H	2-phenylethyl	H	1-(3,5-dimethyl)adamantanyl	2.52
3	H	H	H	3-phenylpropyl	H	1-(3,5-dimethyl)adamantanyl	2.20
4	H	H	H	2-(morpholin-4-yl)ethyl	H	1-(3,5-dimethyl)adamantanyl	2.34
5	H	H	H	n-C <sub>3</sub> H <sub>11</sub>	H	(+)-1-(1,2,3,4-tetrahydronaphthyl)	1.62
6	H	H	H	n-C <sub>3</sub> H <sub>11</sub>	H	(-)-1-(1,2,3,4-tetrahydronaphthyl)	3.00
7	H	H	H	2-(morpholin-4-yl)ethyl	H	1-adamantanyl	2.18
8	H	H	H	n-C <sub>3</sub> H <sub>11</sub>	H	1-(adamantanyl)methyl	1.70
9	H	H	H	n-C <sub>3</sub> H <sub>11</sub>	H	(-)-1-(adamantanyl)ethyl	1.15
10	H	H	H	n-C <sub>3</sub> H <sub>11</sub>	H	(+)-1-(adamantanyl)ethyl	2.31
11	H	H	H	n-C <sub>3</sub> H <sub>11</sub>	Me	1-(3,5-dimethyl)adamantanyl	2.30
12	H	H	H	n-C <sub>3</sub> H <sub>11</sub>	C <sub>6</sub> H <sub>5</sub>	1-(3,5-dimethyl)adamantanyl	2.08
13	H	H	H	n-C <sub>3</sub> H <sub>11</sub>	Me	(-)-1-(phenylethyl)	1.43
14	H	H	H	n-C <sub>3</sub> H <sub>11</sub>	Me	1-adamantanyl	2.53
15	H	H	H	n-C <sub>3</sub> H <sub>11</sub>	H	1-(3,5-dimethyl)adamantanyl	1.26
16	Cl	H	H	n-C <sub>3</sub> H <sub>11</sub>	H	1-(3,5-dimethyl)adamantanyl	1.74
17	H	Cl	H	n-C <sub>3</sub> H <sub>11</sub>	H	1-(3,5-dimethyl)adamantanyl	2.02
18	H	H	Cl	n-C <sub>3</sub> H <sub>11</sub>	H	1-(3,5-dimethyl)adamantanyl	1.44
19	Cl	H	H	n-C <sub>3</sub> H <sub>11</sub>	H	(+)-1-(1,2,3,4-tetrahydronaphthyl)	2.08
20	Cl	H	H	n-C <sub>3</sub> H <sub>11</sub>	H	(-)-1-(adamantanyl)ethyl	2.37
21	Cl	H	H	n-C <sub>3</sub> H <sub>11</sub>	H	(+)-1-(adamantanyl)ethyl	2.16
22	H	Cl	H	n-C <sub>3</sub> H <sub>11</sub>	H	(-)-1-(adamantanyl)ethyl	1.42
23	H	Cl	H	n-C <sub>3</sub> H <sub>11</sub>	H	(+)-1-(adamantanyl)ethyl	2.42
24	H	H	H	n-C <sub>3</sub> H <sub>11</sub>	H	1-(3,5-dimethyl)adamantanyl	2.41
25	--	H	H	n-C <sub>3</sub> H <sub>11</sub>	H	1-(3,5-dimethyl)adamantanyl	1.49
26	H	H	--	n-C <sub>3</sub> H <sub>11</sub>	H	1-(3,5-dimethyl)adamantanyl	1.37
27	H	H	H	n-C <sub>3</sub> H <sub>11</sub>	H	1-(3,5-dimethyl)adamantanyl	1.97

\* In mol. 24 atom marked a is nitrogen, in mol. 25 atom marked b is nitrogen and in molecule 26 atom marked c is nitrogen. In molecule 15 atom marked d is sulphur.

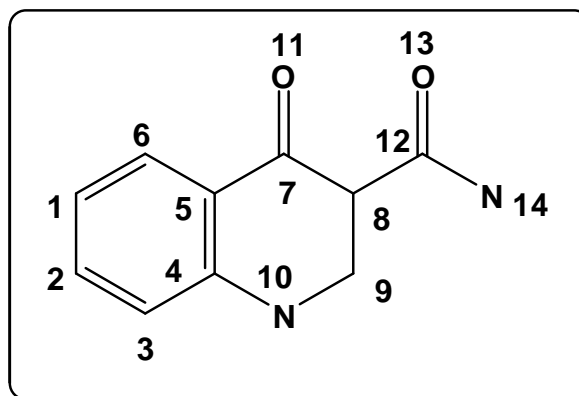


Figure 2. Numbering of atoms used in the LMRA

### Calculations

The electronic structures of all molecules were calculated within Density Functional Theory at the B3LYP/6-311g(d,p) level. The Gaussian suite of programs was used [44]. After full geometry optimization all the information necessary to obtain numerical values for all the electronic local atomic reactivity indices of Eq. 1 was extracted from the Gaussian results with software written in our Unit. Negative electron populations arising from Mulliken Population Analysis were corrected as usual [45]. Molecular orbitals (MO) and Molecular Electrostatic Potentials (MEP) were depicted using GaussView. Orientational parameters were calculated as usual. We made use of LMRA techniques to find the best solution. For each case, a matrix was built containing the dependent variable (the biological activity) and the local atomic reactivity indices of all atoms of the common skeleton as independent variables [29]. The Statistica software was used for the LMRA [46].

### RESULTS

A LMRA including the whole set ( $n=27$ , Table 1) did not produce any statistically significant equation. We then built a new set comprising only those molecules having  $R_3=n$ -pentyl ( $n=22$ ). Consecutive LMRAs showed that molecules 23 and 24 appear as outliers and they were therefore removed from the final set ( $n=20$ ). The best equation obtained was:

$$\log K_i = 11.78 - 0.005S_2^N + 23.96Q_{14} + 8.54F_3(LUMO)^* + 2.37Q_8 - 0.0003\Theta_{R6} \quad (3)$$

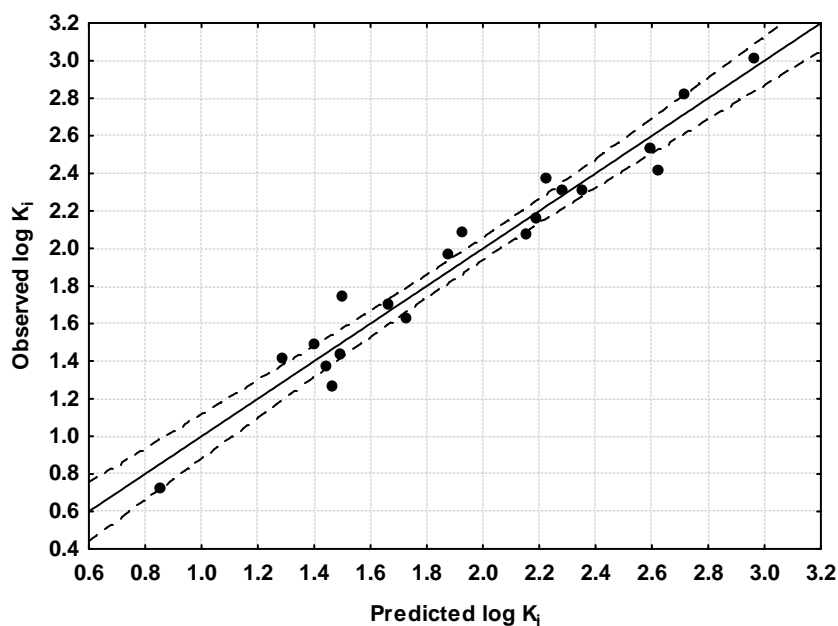
with  $n=20$ ,  $R=0.95$ ,  $\text{adj } R^2=0.94$ ,  $F(5,14)=57.915$  ( $p < 0.000001$ ),  $\text{outliers} > 2\sigma = 0$  and  $SD=0.14$ .  $Q_8$  and  $Q_{14}$  are, respectively, the net charges of atoms 8 and 14 (see Fig. 2 for atom numbering).  $S_2^N$  is the total atomic nucleophilic superdelocalizability of atom 2,  $\Theta_{R6}$  is the orientational parameter of the  $R_6$  substituent and  $F_3(LUMO)^*$  is the Fukui index (*i.e.*, the electron population) of the highest molecular orbital located on atom 3. The beta coefficients and t-test for significance of coefficients of Eq. 3 are shown in Table 2. Concerning independent variables, Table 3 shows that there are no significant internal correlations. Figure 3 shows the plot of observed *vs.* calculated values. The associated statistical parameters of Eq. 5 show that this equation is statistically significant and that the variation of a group of local atomic reactivity indices belonging to the common skeleton explains about 94% of the variation of the CB2 receptor affinity.

Table 2. Beta coefficients and t-test for significance of coefficients in Eq. 3

Variable	Beta	B	t(14)	p-level
$S_2^N$	-0.53	-0.005	-8.78	<0.000001
$Q_{14}$	0.64	23.96	9.94	<0.000001
$F_3(LUMO)^*$	0.66	8.54	9.53	<0.000001
$Q_8$	0.32	2.37	4.96	<0.0002
$\Theta_{R6}$	-0.20	-0.0003	-3.39	<0.0044

Table 3. Squared correlation coefficients for the variables appearing in Eq. 3

	$S_2^N$	$F_3(LUMO)^*$	$Q_8$	$Q_{14}$	$\Theta_{R6}$
$S_2^N$	1.00				
$F_3(LUMO)^*$	0.04	1.00			
$Q_8$	0.007	0.19	1.00		
$Q_{14}$	0.07	0.11	0.0004	1.00	
$\Theta_{R6}$	0.04	0.006	0.0008	0.04	1.00

Figure 3. Plot of predicted vs. observed  $\log(K_i)$  values from Eq. 3. Dashed lines denote the 95% confidence interval

## DISCUSSION

### Molecular Electrostatic Potential

Figure 4 shows the MEP of molecule 19.

We can appreciate that the MEP presents a wide region of positive values around the n-pentyl substituent. The rest of the molecule is surrounded by a region of negative MEP. This MEP structure is representative of all the molecules studied here and could serve as a basis for comparison with more complex systems displaying affinity for the CB2 receptor. For example, Fig. 5 shows the MEP of a 1-aryl-5-(1H-pyrrol-1-yl)-1H-pyrazole-3-carboxamide derivative studied earlier [10].

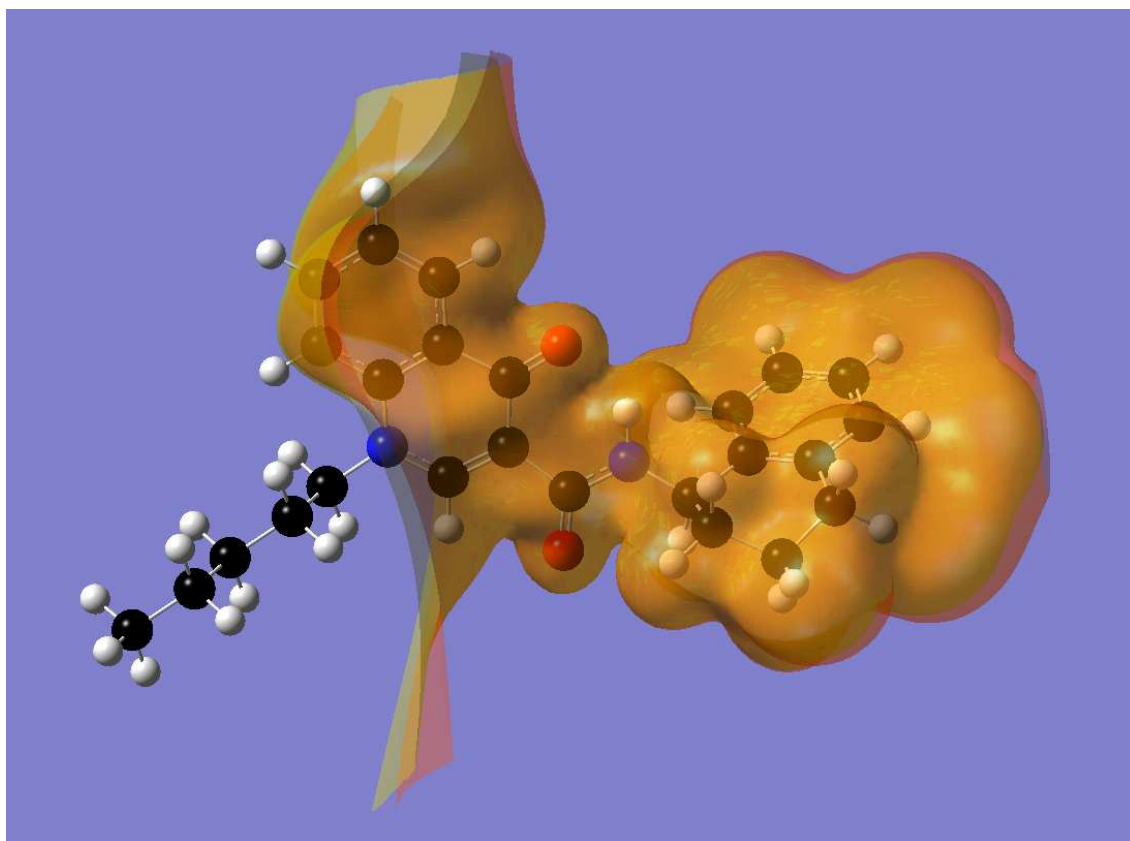


**Figure 4. Molecular electrostatic potential of molecule 19**

*The orange isovalue surface corresponds to negative MEP values (-0.0004) and the yellow isovalue surface to positive MEP values (0.0004)*

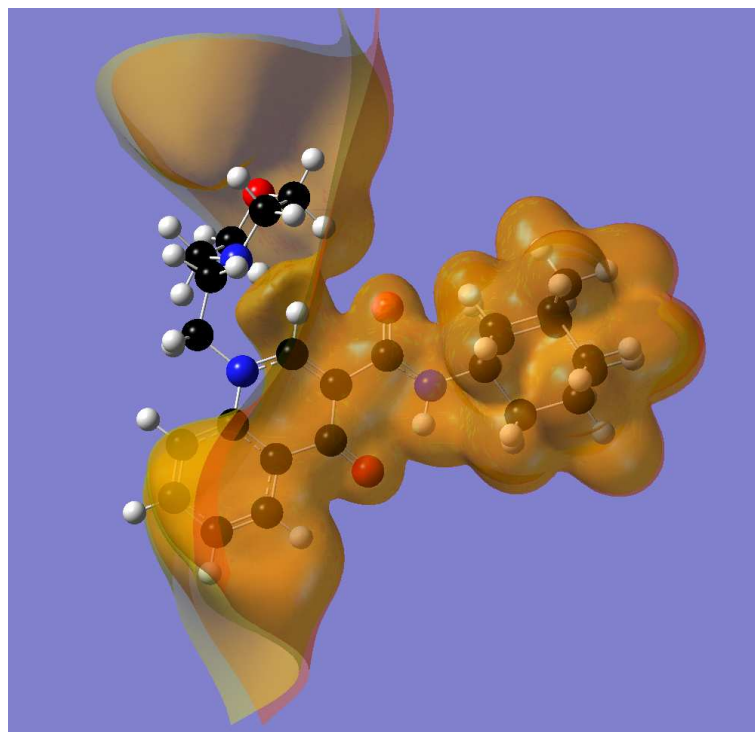


**Figure 5. Molecular electrostatic potential of a 1-aryl-5-(1H-pyrrol-1-yl)-1H-pyrazole-3-carboxamide derivative**

*The orange isovalue surface corresponds to negative MEP values (-0.0004) and the yellow isovalue surface to positive MEP values (0.0004).*

The comparison of Figs. 4 and 5 shows that, despite the difference in their molecular structures, both systems have clearly similar positive and negative MEP regions. Therefore, this similar MEP structure might correspond to that participating in the earlier stages of the drug-receptor recognition process [23,47].



## Molecular Orbital localization

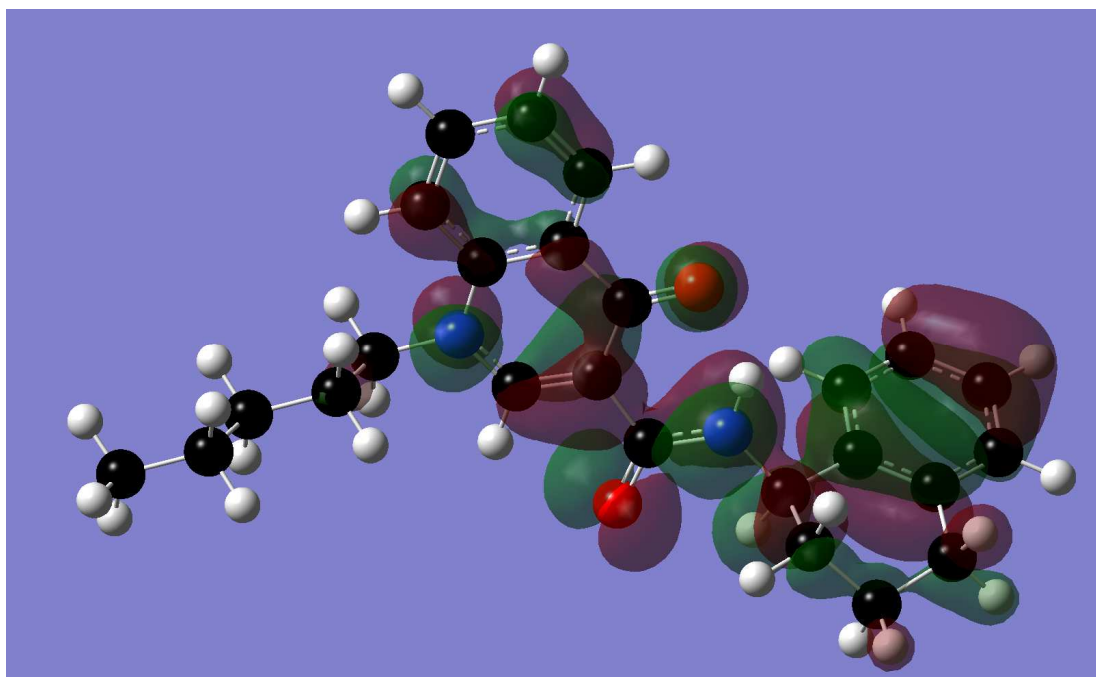


Figure 6. Localization of the highest occupied molecular orbital (HOMO) of molecule 19 (isovalue = 0.02)

We can see in Fig. 6 that the HOMO is mainly of  $\pi$  nature and is localized mainly on the phenyl rings and carbonyl oxygen atoms. Note that the HOMO is not localized on some atoms of the common skeleton rings (for example on atom 2).

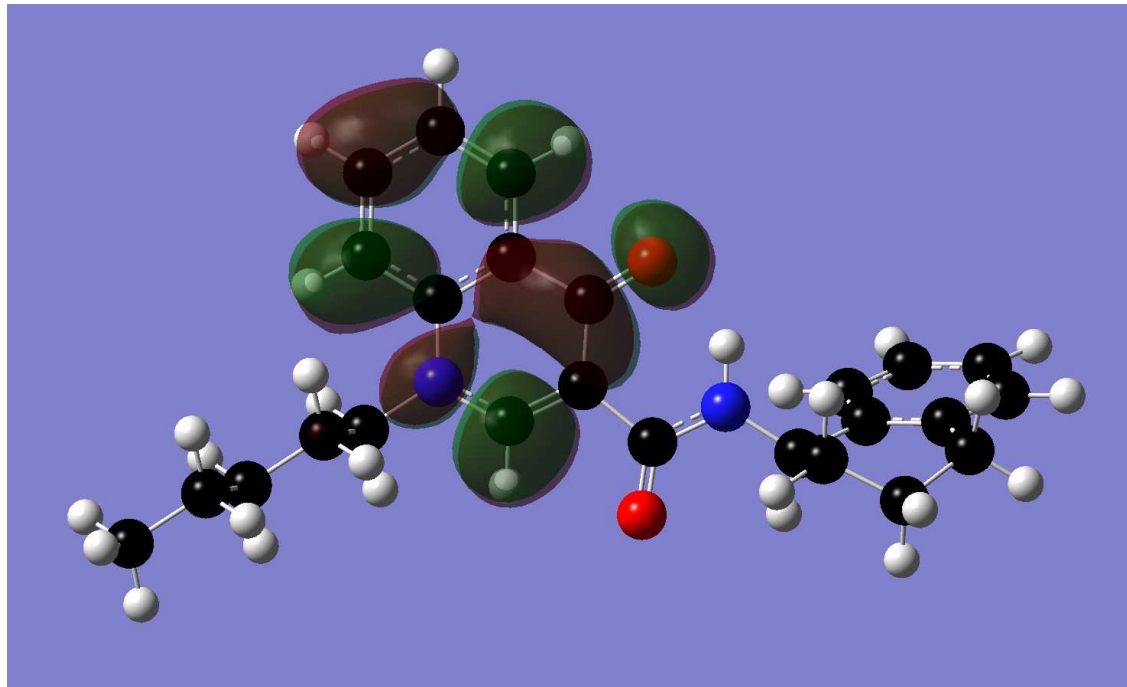


Figure 7. Localization of the lowest empty molecular orbital (LUMO) of molecule 19 (isovalue = 0.02)

The LUMO is localized only on atoms belonging to the common skeleton rings.

**Relationships between electronic structure and receptor binding affinity**

The results reported here indicate that the variation of the hCB2 receptor binding affinity is related to the variation of a set of local atomic reactivity indices belonging to specific atoms of the common skeleton. The results obtained

are very good considering the approximations used to build the model. It is important to point out that, as we are working with the variation of the reactivity indices, the contributions that are constant throughout the series will not appear in the final equation.

The beta values (Table 2) indicate that the importance of variables is  $Q_{14} = F_3(LUMO)^* > S_2^N > Q_8 > \Theta_{R6}$ . Table 3 shows that there is no significant correlation between any pair of variables. Figure 3 shows that only a few points lay just outside the 95% confidence limit. This is a good hint that the common skeleton hypothesis works well for this case. The standard error of estimate is 0.14, a value that is lower than those normally obtained in theoretical studies of 1:1 *in vitro* drug-receptor interaction.

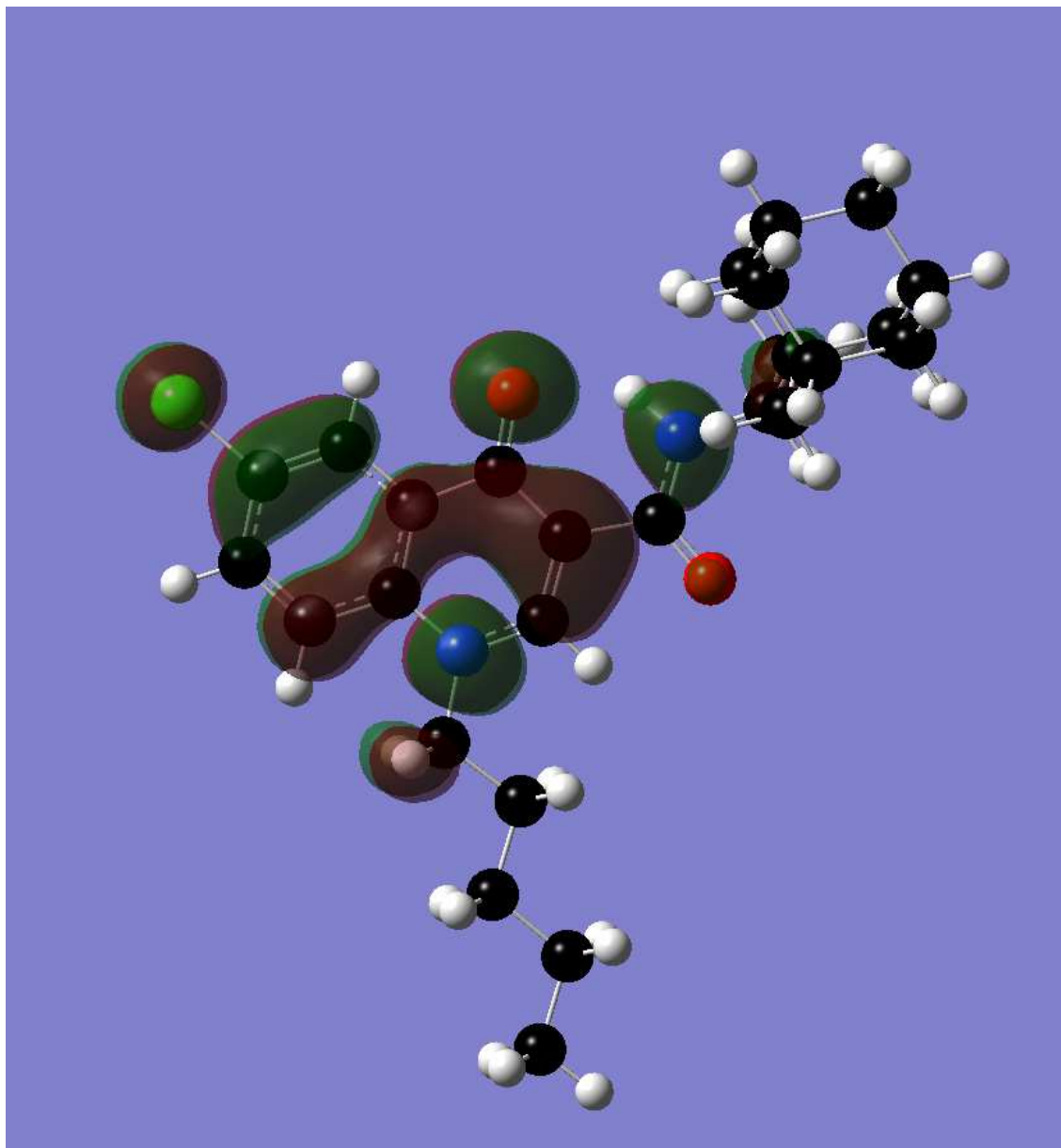


Figure 8. Localization of the highest occupied molecular orbital (HOMO) of molecule 22 (isovalue = 0.02)

A variable-by-variable analysis of Eq. 3 suggests that high hCB2 receptor binding affinity is associated with negative net charges on atoms 8 and 14, a high value for the orientational parameter of the  $R_6$  substituent (Fig. 1), a high value of the local atomic nucleophilic superdelocalizability of atom 2 and a low electron population of the local HOMO\* of atom 3. Net charges on atoms 8 and 14 suggest that an electrostatic interaction occurs with a positively charged area in the hCB2 receptor (such as a guanidinium group for example). Note that in one previous paper a similar area appears involved in electron transfer (see Fig. 15 of Ref. [10]). A high value required for the orientational parameter of  $R_6$  suggests that this moiety could serve for slowing the rotational velocity of the whole



molecule to provide enough time for the recognition process [23]. A similar term also appeared in our earlier work [10]. A high value for  $S_2^N$  indicates that atom 2, alone or as a part of the aromatic system, participates as an electron acceptor center with a counterpart on the receptor. Note that if the HOMO is not localized on atom 2 the process for electron acceptance is facilitated. Figure 6 shows that this is the case for molecule 19. Figure 8 shows the HOMO of molecule 22. This MO is also not localized on atom 2.

Within this analysis, a low electron population of the local HOMO\* of atom 3 could be an indirect indication that the receptor's electron-donor center interacting with atom 2 is a bulky one (a group of neighboring carboxylate or carbonyl groups for example) needing a minimal repulsive interaction with the electrons of atom 3. Figure 9 shows the two dimensional (2D) interaction pharmacophore.

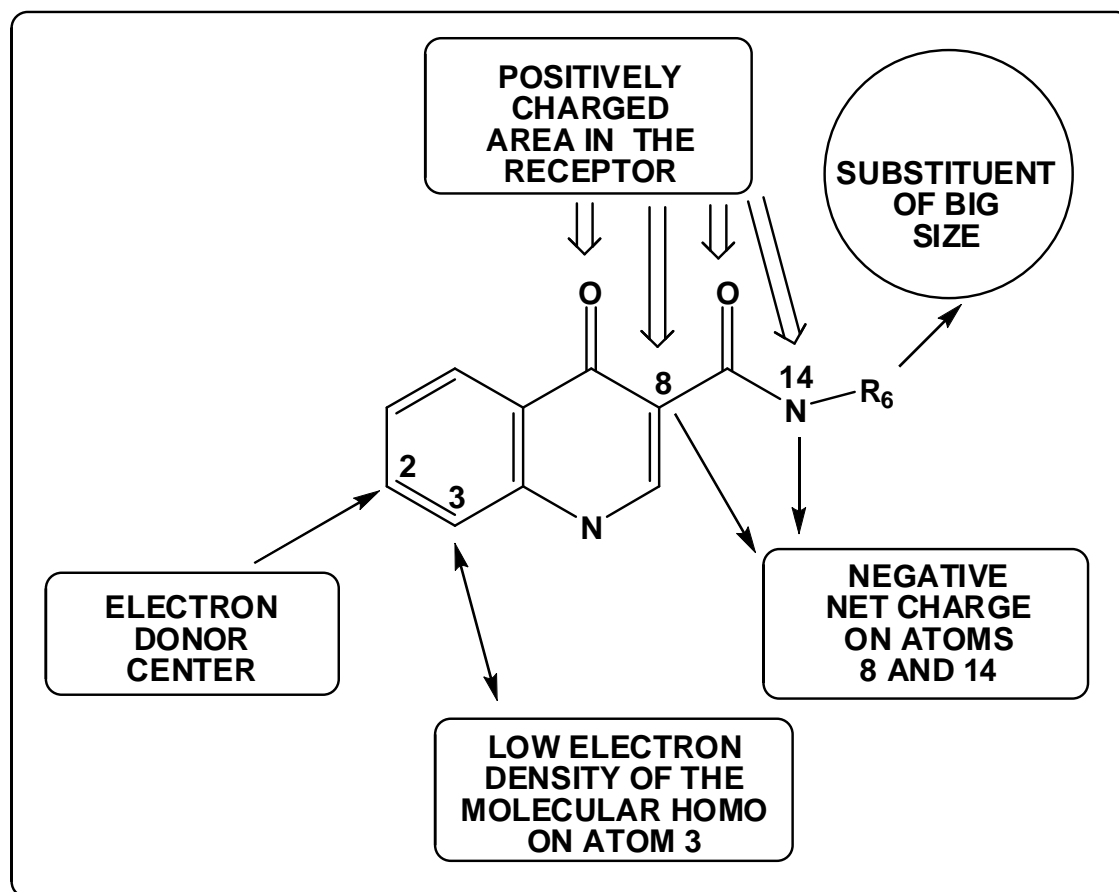


Figure 9. 2D interaction pharmacophore for 4-oxo-1,4-dihydroquinoline-3-carboxamide derivatives

### CONCLUSION

The main conclusions of this work are as follows. 1. We obtained a statistically significant equation relating the variation of hCB2 receptor binding affinities with the variation of a definite set of local atomic reactivity indices. 2. For this case, the interaction of the molecules with the hCB2 receptor is mainly charge-controlled. 3. More studies of different series are needed to expand our knowledge of the CB2 interaction pharmacophore. 4. The common skeleton hypothesis seems to work well enough to be applied in this kind of studies.

### REFERENCES

- [1] RG Pertwee; AC Howlett; ME Abood; SPH Alexander; V Di Marzo; MR Elphick; PJ Greasley; HS Hansen; G Kunos; K Mackie; R Mechoulam; RA Ross, *Pharmacol. Rev.*, **2010**, 62 (4), 588.
- [2] R Mechoulam; LA Parker, *Ann. Rev. Psychol.*, **2013**, 64 (1), 21.
- [3] KD Patel; JS Davison; QJ Pittman; KA Sharkey, *Curr. Med. Chem.*, **2010**, 17 (14), 1394.
- [4] P Marini; M-G Cascio; A King; RG Pertwee; RA Ross, *Brit. J. Pharm.*, **2013**, 169 (4), 887.
- [5] T Nevalainen, *Curr. Med. Chem.*, **2013**,
- [6] YC Martin, *Quantitative drug design: a critical introduction*, M. Dekker, New York, 1978.

- [7] RS Rapaka; A Makriyannis, *Structure-activity relationships of the cannabinoids*, U.S. Dept. of Health and Human Services, Public Health Service, Alcohol, Drug Abuse, and Mental Health Administration, Rockville, MD., Washington, D.C., 1987.
- [8] JS Gómez-Jeria; F Soto-Morales; G Larenas-Gutierrez, *Ir. Int. J. Sci.*, **2003**, 4 (2), 151.
- [9] JS Gómez-Jeria; F Soto-Morales; J Rivas; A Sotomayor, *J. Chil. Chem. Soc.*, **2008**, 53 (1), 1393.
- [10] F Salgado-Valdés; JS Gómez-Jeria, *J. Quant. Chem.*, **2014**, 2014 Article ID 431432 1-15.
- [11] E Stern; GG Muccioli; B Bosier; L Hamtiaux; R Millet; JH Poupaert; J-P Hélichart; P Depreux; J-F Goossens; DM Lambert, *J. Med. Chem.*, **2007**, 50 (22), 5471.
- [12] H-L Li, *Econ Bot*, **1973**, 28 (4), 437.
- [13] EL Abel, *Marihuana, the first twelve thousand years*, McGraw-Hill, New York, 1982.
- [14] ML Ryder, *Environmental Archaeology. J. Hum. Palaeoecol.*, **1999**, 4 (1), 93.
- [15] JP Mallory; VH Mair, *The Tarim mummies: ancient China and the mystery of the earliest peoples from the West*, Thames & Hudson, New York, N.Y., **2000**.
- [16] JH Mills, *Madness, cannabis and colonialism: the 'native only' lunatic asylums of British India, 1857-1900*, St. Martin's Press, New York, **2000**.
- [17] M Booth, *Cannabis: a history*, Picador, New York, **2005**.
- [18] JH Mills; P Barton, *Drugs and empires: essays in modern imperialism and intoxication, c.1500-c.1930*, Palgrave Macmillan, Basingstoke; New York, 2007.
- [19] R Ghosh; P Ganpathy; V Kadam, *Der Pharm. Lett.*, **2010**, 2 (2), 258.
- [20] A Chauhan; PK Sharma; P Srivastava; N Kumar; R Dudhe, *Der Pharm. Lett.*, **2010**, 2 (3),
- [21] JS Gómez-Jeria, *Boll. Chim. Farmac.*, **1982**, 121 (12), 619.
- [22] JS Gómez-Jeria, *Int. J. Quant. Chem.*, **1983**, 23 (6), 1969.
- [23] JS Gómez-Jeria, "Modeling the Drug-Receptor Interaction in Quantum Pharmacology," in *Molecules in Physics, Chemistry, and Biology*, J. Maruani Ed., vol. 4, pp. 215, Springer Netherlands, 1989.
- [24] JS Gómez-Jeria; M Ojeda-Vergara; C Donoso-Espinoza, *Mol. Engn.*, **1995**, 5 (4), 391.
- [25] JS Gómez-Jeria; M Ojeda-Vergara, *J. Chil. Chem. Soc.*, **2003**, 48 (4), 119.
- [26] JS Gómez-Jeria, *J. Chil. Chem. Soc.*, **2010**, 55 (3), 381.
- [27] T Bruna-Larenas; JS Gómez-Jeria, *Int. J. Med. Chem.*, **2012**, 2012 Article ID 682495, 1.
- [28] DA Alarcón; F Gatica-Díaz; JS Gómez-Jeria, *J. Chil. Chem. Soc.*, **2013**, 58 (3), 1651.
- [29] JS Gómez-Jeria, *Elements of Molecular Electronic Pharmacology (in Spanish)*, Ediciones Sokar, Santiago de Chile, 2013.
- [30] JS Gómez-Jeria; M Flores-Catalán, *Canad. Chem. Trans.*, **2013**, 1 (3), 215.
- [31] JS Gómez-Jeria, *Canad. Chem. Trans.*, **2013**, 1 (1), 25.
- [32] JS Gómez-Jeria, "New reactivity indices in discrete and extended systems," PhD in Molecular Physical Chemistry Thesis, pp. 197, UNAB, Santiago de Chile, **2008**.
- [33] JS Gómez-Jeria; D Morales-Lagos, "The mode of binding of phenylalkylamines to the Serotonergic Receptor," in *QSAR in design of Bioactive Drugs*, M. Kuchar Ed., pp. 145, Prous, J.R., Barcelona, Spain, **1984**.
- [34] JS Gómez-Jeria, *Il Far. (Ed. Sci)*. **1985**, 40 (5), 299.
- [35] JS Gómez-Jeria; D Morales-Lagos; JI Rodríguez-Gatica; JC Saavedra-Aguilar, *Int. J. Quant. Chem.*, **1985**, 28 (4), 421.
- [36] JS Gómez-Jeria; D Morales-Lagos; BK Cassels; JC Saavedra-Aguilar, *Quant. Struct.-Relat.*, **1986**, 5 (4), 153.
- [37] JS Gómez-Jeria; P Sotomayor, *J. Mol. Struct. (Theochem)*, **1988**, 166 (C), 493.
- [38] JS Gómez-Jeria; L Lagos-Arancibia, *Int. J. Quant. Chem.*, **1999**, 71 (6), 505.
- [39] JS Gómez-Jeria; L Lagos-Arancibia; E Sobarzo-Sánchez, *Bol. Soc. Chil. Quím.*, **2003**, 48 (1), 61.
- [40] JS Gómez-Jeria; LA Gerli-Candia; SM Hurtado, *J. Chil. Chem. Soc.*, **2004**, 49 (4), 307.
- [41] F Soto-Morales; JS Gómez-Jeria, *J. Chil. Chem. Soc.*, **2007**, 52 (3), 1214.
- [42] A Paz de la Vega; DA Alarcón; JS Gómez-Jeria, *J. Chil. Chem. Soc.*, **2013**, In press.
- [43] I Reyes-Díaz; JS Gómez-Jeria, *J. Comput. Methods Mol. Des.*, **2013**, 3(4), 11.
- [44] MJ Frisch; GW Trucks; H Schlegel et al., *Gaussian98 Rev. A.11.3*, Gaussian, Pittsburgh, PA, USA, 2002.
- [45] JS Gómez-Jeria, *J. Chil. Chem. Soc.*, **2009**, 54 (4), 482.
- [46] Statsoft, *Statistica 8.0*, 2300 East 14 th St. Tulsa, OK 74104, USA, 1984-2007.
- [47] JS Gómez-Jeria, *Acta sud Amer. Quím.*, **1984**, 4 (1), 1.